

Magnetization in a quenched random-bond Ising ferromagnet with anisotropic coupling constants

E. F. Sarmiento

Departamento de Física, Universidade Federal de Alagoas, 57000 Maceió, Al, Brazil

Constantino Tsallis

*Centro Brasileiro de Pesquisas Físicas, Rua Xavier Sigaud, 150, Rio de Janeiro, Brazil
and Departamento de Física, Universidade Federal de Alagoas, 57000 Maceió, Al, Brazil*

(Received 6 May 1982; revised manuscript received 25 August 1982)

Within the framework of an effective-field theory we discuss the phase diagram (ferromagnetic-phase stability limit) and magnetization of a quenched bond-mixed spin- $\frac{1}{2}$ Ising model in an anisotropic simple cubic lattice for both competing and noncompeting interactions. Although analytically simple, the present formalism is superior to the standard mean-field approximation regarding at least two important features, namely, it is capable of providing (i) vanishing critical temperatures for one-dimensional systems, and (ii) expected nonuniform convergences in the highly diluted and highly anisotropic limits. The generality of the model under consideration permits the exhibition of a certain amount of physically interesting crossovers (dimensionality changes, dilute-nondilute behavior, or even mixed situations) at both the phase diagram and magnetization levels. Whenever comparison is possible a satisfactory qualitative (and to a certain extent quantitative) agreement is observed with results available in the literature.

I. INTRODUCTION

During the last decade a considerable theoretical and experimental effort has been dedicated to the study of quenched random magnetic crystalline systems. Two basic problems are usually discussed, namely, the site-random and the bond-random ones; the former has been illustrated through several substances, such as $Mn_pZn_{1-p}F_2$ (Ref. 1), $Rb_2Mn_{1-p}F_4$ (Refs. 2 and 3), $Fe_pMg_{1-p}Cl_2$ (Ref. 4), $Rb_2Co_pMg_{1-p}F_4$ (Ref. 5), $K_2Mn_pFe_{1-p}F_4$ (Ref. 6), $Fe_pCo_{1-p}Cl_2 \cdot 2H_2O$ (Ref. 7), $Fe_pCo_{1-p}Cl_2$ (Ref. 8), $Cd_{1-p}Mn_pTe$ (Ref. 9), among others; although experimentally more complicated, a bond-random-like problem has been exhibited at least in one case, namely, the $Co(S_pSe_{1-p})_2$ (Ref. 10), in which the Co atoms interact essentially through superexchange via the S or Se atoms (thus simulating coupling constants J and J'). Most substances present isotropic or anisotropic Heisenberg-type interactions; however, if a strong uniaxial spin anisotropy (due, for instance, to the crystalline influence) is present, the Ising model can be a convenient representation with the further advantage of being theoretically more tractable. Concerning random versions of this model, several frameworks have been used such as Monte Carlo,^{11,12} high-temperature expansions,^{13,14} variational method,¹⁵ perturbative methods¹⁶⁻²²

(effective-medium, coherent-potential, random-phase approximations), duality and/or replica trick arguments,²³⁻²⁹ exact arguments,³⁰ and renormalization-group approaches³¹⁻⁴⁰ among others (see also Ref. 41).

Recently Honmura and Kaneyoshi⁴² presented, for the Ising model, a new type of effective-field theory which, without introducing mathematical complexities, substantially improves on the standard mean-field approximation (MFA). This framework (see Ref. 43 for a pedagogical version), based in the introduction of a differential operator into the exact spin-correlation-function identity obtained by Callen,⁴⁴ provides in particular a vanishing critical temperature for one-dimensional systems as well as nontrivial nonuniform convergences in complex phase diagrams; it is well known that the MFA fails in recovering this type of results. This procedure shares with the MFA a great versatility and has already been applied to several situations such as pure,⁴⁵⁻⁴⁷ site-random,⁴⁸ bond-random⁴⁹⁻⁵² Ising bulk problems as well as surface ones.^{53,54}

All three Refs. 50-52 refer to the quenched bond-mixed spin- $\frac{1}{2}$ isotropic Ising model (the nearest-neighbor coupling constant associated with each bond is assumed to take values J or J' with arbitrary concentrations; $\alpha \equiv J'/J$); in Ref. 50 the vanishing-temperature square-lattice problem for

$\alpha = -1$ (competing interactions) is discussed; the extension to all temperatures and all values of α (i.e., noncompeting as well as competing interactions) is performed in Ref. 51. Finally in Ref. 52 we present a preliminary report concerning the finite-temperature simple cubic lattice problem for noncompeting interactions ($\alpha \geq 0$).

In the present paper we follow along the lines of the three preceding references and consider, for all temperatures, the *anisotropic* simple cubic lattice problem for noncompeting as well as competing interactions. Two (mutually nonexclusive) main sources of crystalline anisotropy may exist, namely, anisotropic coupling constants or anisotropic bond occupancy probabilities; we are herein particularly concerned with the former (the latter will be the subject of a forthcoming paper). We calculate the spontaneous magnetization as a function of temperature and bond concentration for a large class of cases and specifically exhibit the most interesting situations (in particular, those related to linear chain \leftrightarrow square lattice \leftrightarrow cubic lattice crossovers). By imposing the condition of vanishing magnetization, we obtain the critical surfaces associated with the ferromagnetic-phase stability limit (within the present theory the ferroparamagnetic phase transitions are obtained to be of the second-order one in agreement with common expectations; the discussion of eventual ferromagnetic \leftrightarrow spin-glass phase transitions at relatively low temperatures are beyond the scope of the present work). All the phase diagrams appearing in Refs. 50–52 are herein recovered as particular cases.

In Sec. II we introduce the general model we are interested in as well as the theoretical framework within which we discuss it; in Sec. III we treat a great amount of important particular cases; the overall conclusions are presented in Sec. IV.

II. MODEL AND FORMALISM

Let us consider a system whose Hamiltonian is given by

$$\mathcal{H} = - \sum_{\langle i,j \rangle} J_{ij} \sigma_i \sigma_j \quad (\sigma_i, \sigma_j = \pm 1), \quad (1)$$

where $\langle i,j \rangle$ runs over all the nearest-neighboring

$$\begin{aligned} \langle \sigma_i \rangle = & \left[\sum_{j=1}^6 \left(\langle \sigma_j \rangle \sinh(\beta J_{ij} D) \prod_{k \neq j} \cosh(\beta J_{ik} D) \right. \right. \\ & + \frac{1}{3!} \sum_{k \neq j} \sum_{l \neq j, k} \langle \sigma_j \sigma_k \sigma_l \rangle \sinh(\beta J_{ij} D) \sinh(\beta J_{ik} D) \sinh(\beta J_{il} D) \prod_{m \neq j, k, l} \cosh(\beta J_{im} D) \\ & \left. \left. + \frac{1}{5!} \sum_{k \neq j} \sum_{l \neq j, k} \sum_{m \neq j, k, l} \sum_{n \neq j, k, l, m} \langle \sigma_j \sigma_k \sigma_l \sigma_m \sigma_n \rangle \right) \right] \end{aligned}$$

couples of sites of a simple cubic lattice; J_{ij} is a random variable associated with three different distribution laws along the three crystalline directions (denoted by 1, 2, and 3), namely,

$$P_r(J_{ij}) = (1-p_r)\delta(J_{ij}-J'_r) + p_r\delta(J_{ij}-J_r) \quad (r=1,2,3), \quad (2)$$

where we assume $0 \leq p_r \leq 1$ ($\forall r$), $0 \leq J_1 \leq J_2 \leq J_3 > 0$ and $J'_r \leq J_r$ ($\forall r$). Note that by imposing these conditions we are not physically restricting the model (we recall in particular that in the simple cubic lattice, all other choices of the signs of $\{J_r\}$ correspond to models which are isomorphic to the ferromagnetic one we are considering here).

Before going on let us introduce the following convenient notation:

$$\begin{aligned} \alpha_r &\equiv J'_r / J_3 \quad (r=1,2,3), \\ \gamma_q &\equiv J_q / J_3 \quad (q=1,2), \end{aligned} \quad (3)$$

where we can verify that $0 \leq \gamma_1 \leq \gamma_2 \leq 1$, $\alpha_1 \leq \gamma_1$, $\alpha_2 \leq \gamma_2$, and $\alpha_3 \leq 1$.

The starting point for the statistics of our Ising spin system is the following Callen⁴⁴ identity (see also Ref. 55):

$$\langle \sigma_i \rangle = \left\langle \tanh \beta \sum_j J_{ij} \sigma_j \right\rangle, \quad (4)$$

where $\beta \equiv 1/k_B T$, $\langle \dots \rangle$ indicates the canonical *thermal* average for a given configuration of the $\{J_{ij}\}$, and j runs over the nearest neighbors of the site i . Following Honmura and Kaneyoshi⁴² we introduce the differential operator $D \equiv \partial/\partial x$ into relation (4) and obtain

$$\begin{aligned} \langle \sigma_i \rangle = & \left\langle \exp \left[\beta D \sum_j J_{ij} \sigma_j \right] \tanh x \right|_{x=0} \\ = & \left\langle \prod_j [\cosh(\beta D J_{ij}) \right. \\ & \left. + \sigma_j \sinh(\beta D J_{ij})] \right\rangle \tanh x \Big|_{x=0}. \end{aligned} \quad (5)$$

When applied to our model this relation may be, through tedious but straightforward algebra, rewritten in the following compact form:

$$\begin{aligned} & \times \sinh(\beta J_{ij} D) \sinh(\beta J_{ik} D) \sinh(\beta J_{il} D) \sinh(\beta J_{im} D) \sinh(\beta J_{in} D) \\ & \times \prod_{p \neq j, k, l, m, n} \cosh(\beta J_{ip} D) \Bigg] \Bigg| \tanh x \Big|_{x=0}, \end{aligned} \quad (6)$$

where the subscripts run from 1 to 6 in order to refer to the six nearest-neighbor sites of the i th one, and where we have used the property $f(D) \tanh x \Big|_{x=0} = 0$ valid for any even function $f(D)$. Note that the *exact* equation (6) yields a set of relations between the magnetization of the i th site and associated multispin correlation functions once the bond configuration $\{J_{ij}\}$ is completely specified.

The central scope of this work is to estimate, from Eq. (6) and for arbitrary values of the temperature and the bond concentration, the spontaneous magnetization of the system, and to extract from this knowledge the critical frontier which separates the ferromagnetic phase from any other (to be more precise, we intend to determine the limit of stability of the long-range ferromagnetic order). It is clear that, if we try to exactly treat all the spin-spin correlations present in Eq. (6) and to properly perform the configurational averages which are still to be done, the problem becomes mathematically untractable (see also Ref. 55). We shall therefore proceed as follows: We take on both sides of Eq. (6) the configurational average (denoted by $\langle \dots \rangle_J$), then completely decouple the multispin correlation functions and use the fact that our model is a quenched one and therefore the distribution laws associated with different bonds are independent among them. It is clear that within these approximations (where spin-spin correlations are neglected), the strict criticality of the system is lost (in particular, the critical exponents are going to be the classical ones, and the real dimensionality of the system is only partially taken into account through the coordination number z); nevertheless, the present framework is, as already mentioned, quite superior to the standard MFA: this point has already been verified in several models⁴⁵⁻⁵⁴ and, for the present one, will be exhibited further on. The magnetization satisfies

$$\langle \langle \sigma_i \rangle \rangle_J \equiv m = 2Am + 2Bm^3 + 2Cm^5, \quad (7)$$

with

$$A \equiv (s_1 c_1 c_2^2 c_3^2 + s_2 c_2 c_3^2 c_1^2 + s_3 c_3 c_1^2 c_2^2) \tanh x \Big|_{x=0}, \quad (8)$$

$$\begin{aligned} B \equiv & [s_1 c_1 (s_2^2 c_3^2 + s_3^2 c_2^2) + s_2 c_2 (s_3^2 c_1^2 + s_1^2 c_3^2) \\ & + s_3 c_3 (s_1^2 c_2^2 + s_2^2 c_1^2) \\ & + 4s_1 s_2 s_3 c_1 c_2 c_3] \tanh x \Big|_{x=0}, \end{aligned} \quad (9)$$

$$C \equiv (s_1 c_1 s_2^2 s_3^2 + s_2 c_2 s_3^2 s_1^2 + s_3 c_3 s_1^2 s_2^2) \tanh x \Big|_{x=0}, \quad (10)$$

where

$$\begin{aligned} s_r & \equiv \langle \sinh(\beta J_{ij} D) \rangle_J \\ & = (1-p_r) \sinh(\beta J'_r D) + p_r \sinh(\beta J_r D) \end{aligned} \quad (r=1,2,3) \quad (11)$$

and

$$\begin{aligned} c_r & \equiv \langle \cosh(\beta J_{ij} D) \rangle_J \\ & = (1-p_r) \cosh(\beta J'_r D) + p_r \cosh(\beta J_r D) \end{aligned} \quad (r=1,2,3), \quad (12)$$

where we have explicitly used the distribution laws (2). Equation (7) admits two solutions, namely, $m \equiv 0$ (nonferromagnetic phase) and a nontrivial one (associated with the ferromagnetic phase) given by

$$m = \left[\frac{-B - [B^2 - 2C(2A - 1)]^{1/2}}{2C} \right]^{1/2}. \quad (13)$$

The critical surface characterizing the ferromagnetic-phase stability limit is determined by $m = 0$, hence

$$2A = 1. \quad (14)$$

We can verify in all physically meaningful cases that $B \leq 0$ and $C \geq 0$ and that $A > \frac{1}{2}$ ($A < \frac{1}{2}$) in the ferromagnetic (nonferromagnetic) phase; these facts are related to the second-order phase-transition behavior of the magnetization we have observed (several illustrations are presented further on). We can also verify that the square lattice case ($J'_1 = J_1 = 0$) leads to $C = 0$ and

$$A = (s_2 c_2 c_3^2 + s_3 c_3 c_2^2) \tanh x \Big|_{x=0}, \quad (15)$$

$$B = (s_2 c_2 s_3^2 + s_3 c_3 s_2^2) \tanh x \Big|_{x=0}, \quad (16)$$

and that the linear-chain case ($J'_1 = J_1 = J'_2 = J_2 = 0$) leads to $B = C = 0$ and

$$A = s_3 c_3 \tanh x \Big|_{x=0}. \quad (17)$$

This last situation deserves a few comments. By replacing Eq. (17) into Eq. (14) we obtain

$$\begin{aligned} (1-p_3)^2 \tanh 2\beta J'_3 + 2p_3(1-p_3) \tanh \beta (J_3 + J'_3) \\ + p_3^2 \tanh 2\beta J_3 = 1. \end{aligned} \quad (18)$$

We remark that (a) in the case $J'_3 > 0$ (we recall that $J'_3 \leq J_3 > 0$ by convention) the unique solution is $T_c = 0$ and it exists for all values of p , and (b) in the case $J'_3 \leq 0$ the unique solution is $(p, T_c) = (1, 0)$. Both predictions of this theory are *exact* as it is well known.

As anticipated this is a substantial improvement on MFA, which can be herein recovered (see, for example, Ref. 54) by introducing in Eq. (18) $\tanh x \simeq x$, which, if $J'_3 \geq 0$, leads to

$$k_B T_c^{\text{MFA}} = 2[(1-p_3)J'_3 + p_3 J_3], \quad (19)$$

and, if $J'_3 < 0$, leads to

$$k_B T_c^{\text{MFA}} = \begin{cases} 0 & \text{if } p \leq p_c \\ 2[-(1-p_3)|J'_3| + p_3 J_3] & \text{if } p > p_c, \end{cases} \quad (20)$$

where $p_c \equiv |J'_3| / (|J'_3| + J_3)$. All these results exhibit the well-known failure of MFA-type theories for one-dimensional short-range-forces systems.

The model introduced in Eqs. (1) and (2) is very

general and the magnetization is a function

$$m(t, p_1, p_2, p_3; \alpha_1, \alpha_2, \alpha_3, \gamma_1, \gamma_2),$$

where $t \equiv k_B T / J_3$; the stability limit we are interested in corresponds to an eight-dimensional hypersurface in a nine-dimensional parameter space. It is therefore clear that we must restrict ourselves to the (sequential) discussion of many particular cases. In the present paper we will be concerned with the model which is isotropic in the bond-occupancy probabilities (i.e., $p_1 = p_2 = p_3 \equiv p$). In a forthcoming paper we shall present another set of important particular cases corresponding to general values of $\{p_r\}$.

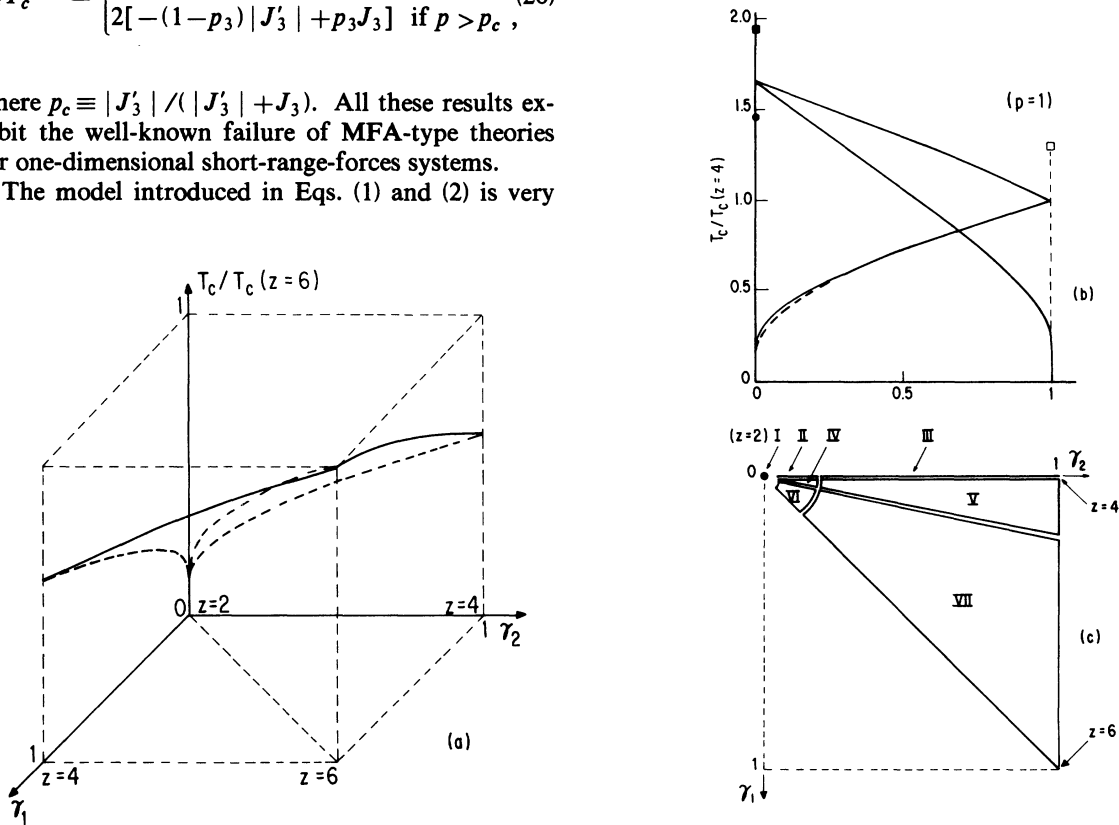


FIG. 1. Critical reduced temperature of the pure ($p=1$) ferromagnet in anisotropic simple cubic lattice ($z=6$). (a) $t_c \equiv k_B T_c / J_3$ as a function of $\gamma_1 \equiv J_1 / J_3$ and $\gamma_2 \equiv J_2 / J_3$. (b) $T_c / T_c(z=4)$ along convenient lines, namely, $\gamma_1 = 0$ and $\gamma_2 \in [0, 1]$ [exhibition of the crossover between $d=1(z=2)$ and $d=2(z=4)$], $\gamma_2 = 1$ and $\gamma_1 \in [0, 1]$ [exhibition of the crossover between $d=2(z=4)$ and $d=3(z=6)$], and finally $\gamma_1 = \gamma_2 \in [0, 1]$ [exhibition of the crossover between $d=1(z=2)$ and $d=3(z=6)$]; for square lattice the exact result (Ref. 56) $\tanh J_3 / k_B T_c = \exp(-2J_2 / k_B T_c)$ (dashed line) as well as the MFA one (\square) are indicated as well; for simple cubic lattice the series (\bullet) (Ref. 57) and MFA (\blacksquare) are also indicated. (c) We have indicated (out of scale) in the (γ_1, γ_2) space the physically interesting (and nonequivalent) situations, namely: I, associated with $\gamma_1 = \gamma_2 = 0$ ($d=1$); II, associated with $\gamma_1 = 0$ and $0 < \gamma_2 \ll 1$ (crossover $d=1 \leftrightarrow d=2$); III, associated with $\gamma_1 = 0$ and $0 < \gamma_2 \leq 1$ ($d=2$ region; in particular, $\gamma_2 = 1$ corresponds to the pure $d=2$ isotropic model); IV, associated with $0 < \gamma_1 \ll \gamma_2 \ll 1$ (sequence of crossovers $d=1 \leftrightarrow d=2 \leftrightarrow d=3$); V, associated with $0 < \gamma_1 \ll \gamma_2 \leq 1$ (crossover $d=2 \leftrightarrow d=3$); VI, associated with $0 < \gamma_1 \leq \gamma_2 \ll 1$ (crossover $d=1 \leftrightarrow d=3$); VII, associated with $0 < \gamma_1 \leq \gamma_2 \leq 1$ ($d=3$ region; in particular, $\gamma_1 = \gamma_2 = 1$ corresponds to the pure $d=3$ isotropic model).

III. PARTICULAR CASES: RESULTS AND DISCUSSION

Herein we intend to present and discuss the results (phase diagrams and magnetization) corresponding to several interesting models (within the restriction $p_1=p_2=p_3\equiv p$ as anticipated).

A. Pure anisotropic models

These models correspond to the particular situation $p=1$, $\forall J_1, J_2, J_3$ (i.e., $\forall \alpha_1, \alpha_2, \alpha_3$) or equivalently $\alpha_1=\gamma_1$, $\alpha_2=\gamma_2$, and $\alpha_3=1\forall p$. The associated phase diagram in the (γ_1, γ_2, t) space is presented in Fig. 1.

The critical temperature associated with $z=2$ (which corresponds to a linear chain, i.e., $d=1$) is obtained by imposing $\gamma_1=\gamma_2=0$: It vanishes in agreement with rigorous arguments [we recall that the MFA leads to $t_c^{\text{MFA}}(z=2)=2$]. The critical temperature associated with $z=4$ (which within the present description corresponds to the square lattice, i.e., $d=2$), is obtained by imposing $\gamma_1=0$ and $\gamma_2=1$; it satisfies the equation

$$\tanh \frac{4}{t_c} + 2 \tanh \frac{2}{t_c} = 2,$$

hence $t_c(z=4)\simeq 3.0898$, which is to be compared with the exact result $t_c^{\text{exact}}=2.2692\dots$ [MFA leads to $t_c^{\text{MFA}}(z=4)=4$]. The present value for t_c coincides with those obtained in Refs. 42, 51, 58–60. Finally, the simple cubic lattice ($z=6$; $d=3$) herein corresponds to $\gamma_1=\gamma_2=1$; its critical point satisfies (in agreement with Ref. 49)

$$\tanh \frac{6}{t_c} + 4 \tanh \frac{4}{t_c} + 5 \tanh \frac{2}{t_c} = \frac{16}{3},$$

which leads to $t_c(z=6)\simeq 5.0733$ [to be compared with $t_c^{\text{series}}\simeq 4.5112$ (Ref. 57), and with $t_c^{\text{MFA}}(z=6)=6$]. We remark in both $z=4$ and $z=6$ cases that the present framework tends to *overestimate* (however, quite less than the MFA) the critical temperatures: This fact comes from the negligence of multispin correlations. We shall come back to this point in Sec. III B 3.

Let us now discuss $T_c(\gamma_1, \gamma_2)$ in the neighborhoods of the points $z=2, 4$, and 6 [see Figs. 1(a) and 1(b)]. Along the line $\gamma_1=0$ we obtain

$$\frac{1}{T_c(0,1)} \frac{dT_c(0, \gamma_2)}{d\gamma_2} \Big|_{\gamma_2=1} = \frac{1}{2} \quad (21)$$

and, in the limit $\gamma_2 \rightarrow 0$ (hence $t_c \rightarrow 0$),

$$\gamma_2 \sim 2t_c e^{-4/t_c}. \quad (22)$$

The exact critical line associated with $\gamma_1=0$ is

well known⁵⁶ and given by

$$\tanh t_c^{-1} = \exp(-2\gamma_2/t_c),$$

which leads to the result indicated in Eq. (21) [which is therefore *exact* and responsible for the good agreement between dashed and solid lines in Fig. 1(b)] as well as to $\gamma_2 \sim t_c e^{-2/t_c}$ in the limit $\gamma_2 \rightarrow 0$. The discrepancy we observe between this asymptotic behavior and the one appearing in Eq. (22) is such that, as before and for the same reason, the corresponding critical temperature is overestimated.

Along the line $\gamma_1=\gamma_2$ we obtain

$$\frac{1}{T_c(1,1)} \frac{dT_c(\gamma_1, \gamma_1)}{d\gamma_1} \Big|_{\gamma_1=1} = \frac{2}{3} \quad (23)$$

and, in the limit $\gamma_1 \rightarrow 0$ (hence $t_c \rightarrow 0$),

$$\gamma_1 \sim t_c e^{-4/t_c}. \quad (24)$$

The value $\frac{2}{3}$ can be compared with 1, obtained for both MFA and series (from Ref. 6).

Finally, along the line $\gamma_2=1$ we obtain

$$\frac{1}{T_c(0,1)} \frac{dT_c(\gamma_1, 1)}{d\gamma_1} \Big|_{\gamma_1=0} \simeq 0.7968 \quad (25)$$

and

$$\frac{1}{T_c(1,1)} \frac{dT_c(\gamma_1, 1)}{d\gamma_1} \Big|_{\gamma_1=1} = \frac{1}{3}. \quad (26)$$

The value 0.7968 can be compared with $\frac{1}{2}$ (MFA), 1 (Bethe-Peierls approximation⁶²) and the much larger value ($\simeq 4$) given by series calculations.^{61,62} Finally, the value $\frac{1}{3}$ can be compared with the MFA value (also $\frac{1}{3}$), the Bethe-Peierls approximation one ($\simeq 0.203$ from Ref. 62), and the series ones ($\simeq 0.345$ from Ref. 61 and $\simeq 0.366$ from Ref. 62).

Concerning the distinct physical regions schematically indicated in Fig. 1(c), let us clarify a few points. Region I is a single point (and corresponds to the strictly one-dimensional model); regions II (quasi-one-dimensional models) and III (fully-two-dimensional models) are linear; regions IV, V, and VI are very small in surface (IV and VI correspond to quasi-one-dimensionality and V to quasi-two-dimensionality); and the (big) region VII corresponds to full three dimensionality. In region II (region VI) the general behavior is typically one dimensional, except for quite low temperatures where the two dimensionality (three dimensionality) is expected to emerge; in region III (region VII) no such $d=1 \leftrightarrow d=2$ ($d=1 \leftrightarrow d=3$) crossover exists. Analogously in region V the behavior is typically

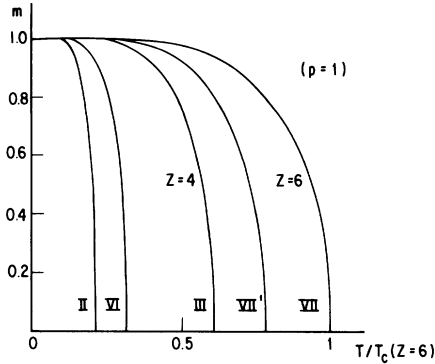


FIG. 2. Examples of the thermal behavior of the reduced magnetization for the pure ($p=1$) ferromagnet in anisotropic simple cubic lattice. The roman numbers are associated with the regions appearing in Fig. 1(c), and herein, respectively, correspond to $\{\gamma_1, \gamma_2\} = \{(0, 0.05); (0.1, 0.1); (0, 1); (0.4, 1); (1, 1)\}$ for the curves II, VI, III, VII', and VII.

two dimensional except for quite low temperatures where the three dimensionality will emerge; no such $d=2 \leftrightarrow d=3$ crossover exists in region VII. Region IV is particularly interesting: One-dimensional behavior is expected for intermediate temperatures (comparable with J_3), two-dimensional behavior is expected for quite low temperatures, whereas three dimensionality will emerge at much lower temperatures. Later on these facts will be specifically illustrated, in particular by considering diluted systems.

In Fig. 2 we present several examples of the thermal behavior of the magnetization. We can follow therein the progression from the $z=2$ case (where $m=1$ for $T=0$, and $m=0$ otherwise) to the $z=6$ case (isotropic simple cubic lattice pure ferromagnet) passing through the $z=4$ case (isotropic square lattice pure ferromagnet). The $z=6$ case has also been discussed in Ref. 49.

B. Random-bond isotropic models

This family of random-bond models correspond to the particular situation where all axes are equivalent in what concerns the coupling constants.

1. Linear chain ($z=2$)

Herein we consider $J_1=J_2=J'_1=J'_2=0$ and $J'_3 \leq J_3$ ($\alpha \equiv J'_3/J_3 \leq 1$). The associated phase diagram has already been discussed in Sec. II: We recall that $\alpha > 0$ implies $T_c=0, \forall p \in [0, 1]$, and that $\alpha \leq 0$ implies that the critical frontier is reduced to the single point $(p, T_c) = (1, 0)$. The magnetization is given, in the case $\alpha > 0$, by

$$m = \begin{cases} 1 & \text{if } T=0, \forall p \in [0, 1] \\ 0 & \text{otherwise,} \end{cases} \quad (27)$$

and, in the case $\alpha \leq 0$, by

$$m = \begin{cases} 1 & \text{if } T=0 \text{ and } p=1 \\ 0 & \text{otherwise.} \end{cases} \quad (28)$$

All these results are well known to be exact.

2. Square lattice ($z=4$)

Herein we consider $J_1=J'_1=0$ and $J'_2=J'_3 \equiv J'_0 \leq J_2=J_3 \equiv J_0$ ($\alpha \equiv J'_0/J_0$). The associated phase diagram is presented in Ref. 51. In the present section we discuss the magnetization as a function of temperature and J_0 -bond concentration. The magnetization is given by $m = [(1-2A)/2B]^{1/2}$.

The condition (14) determines the critical surface in the (p, t, α) space (see Fig. 3). The critical line associated with the bond-diluted model ($\alpha=0$) is given by

$$4(1-p)^3 p \tanh \frac{1}{t_c} + 6(1-p)^2 p^2 \tanh \frac{2}{t_c} + 3(1-p)p^3 \left[\tanh \frac{3}{t_c} + \tanh \frac{1}{t_c} \right] + \frac{1}{2} p^4 \left[\tanh \frac{4}{t_c} + 2 \tanh \frac{2}{t_c} \right] = 1, \quad (29)$$

which provides a bond-percolation critical probability $p_c \equiv p_c(\alpha=0) \simeq 0.4284$. This value coincides with that obtained in Ref. 55 and is to be compared with

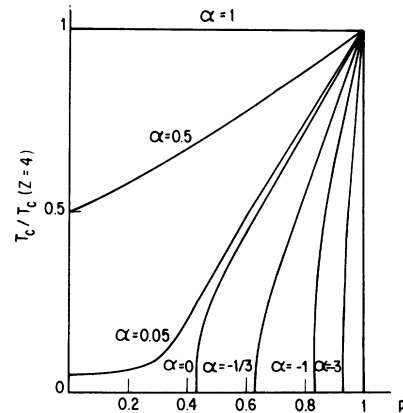


FIG. 3. Examples of critical lines (ferromagnetic-phase stability limit) associated with the quenched random-bond Ising model in square lattice ($z=4$) for both competing ($\alpha \equiv J'_0/J_0 < 0$) and noncompeting ($\alpha \geq 0$) cases.

$p_c^{\text{exact}} = \frac{1}{2}$ (Ref. 63) and with $p_c^{\text{MFA}} = 0$. Within the present framework the square lattice ordered (ferromagnetic) phase is overstabilized (and consequently p_c is underestimated: as already mentioned this is related to the negligence of multispin correlations. Equation (29) also yields

$$\frac{1}{T_c(1)} \left. \frac{dT_c(p)}{dp} \right|_{p=1} \simeq 1.345 \quad (30)$$

and

$$(1-p_c) \left. \frac{de^{-2/t_c(p)}}{dp} \right|_{p=p_c} \simeq 1.156. \quad (31)$$

The first result is to be compared with the exact value¹³ 1.329... and the second one with the exact value²³ 1.386... Let us stress that it is rather remarkable that a simple effective-field theory is capable of providing the exact asymptotic forms for the critical line *simultaneously* in both limits $T \rightarrow 0$ and $p \rightarrow 1$.

The critical lines associated with $0 < \alpha < 1$ present (see Fig. 3), as expected,³⁸ a nonuniform convergence in the limit $\alpha \rightarrow 0$.

Let us now discuss the phase diagrams associated with $\alpha < 0$. At $T=0$ we obtain, respectively, for $\alpha = -\frac{1}{3}, -1, -3$ the following results: $p_c(\alpha = -\frac{1}{3}) \simeq 0.6346$, $p_c(\alpha = -1) = \frac{5}{6}$, and $p_c(\alpha = -3) \simeq 0.9308$.

The value $p_c(\alpha = -1) = \frac{5}{6}$ corresponds to a concentration of antiferromagnetic bonds equal to $\frac{1}{6} \simeq 0.1667$; this value compares well with 0.15–0.20 (Monte Carlo³¹), 0.166 (replica method⁶⁴), 0.167

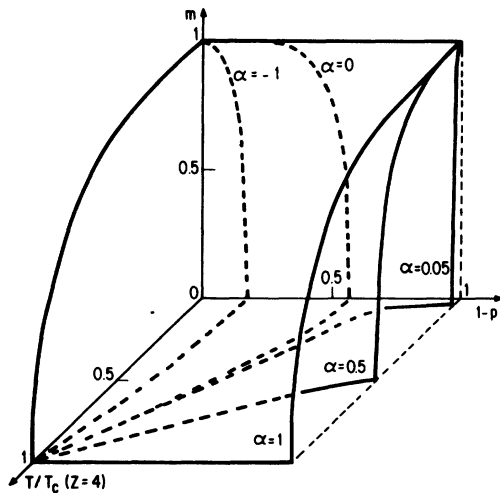


FIG. 4. Influence of $\alpha \equiv J'_0/J_0$ on the magnetization as a function of temperature and concentration for the quenched random-bond Ising model in square lattice ($z=4$). Notice the nonuniform convergence of the family of surfaces in the limit $\alpha \rightarrow 0$.

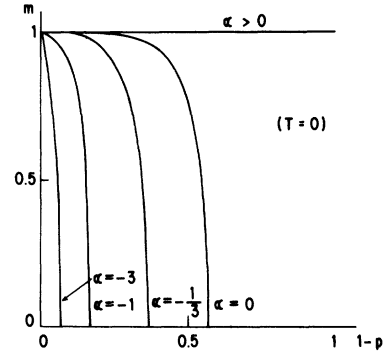


FIG. 5. $T=0$ section of the family of surfaces represented in Fig. 4 for various values of $\alpha \equiv J'_0/J_0$.

(Bethe method⁶⁵), whereas other methods^{66–68} provide a lower value ($\simeq 0.1$). For negative values of α other than $-\frac{1}{3}, -1$, and -3 , the present treatment provides a curious situation at $T=0$ as it leads to $p_c(0 > \alpha > -\frac{1}{3}) \simeq 0.600$, $p_c(-\frac{1}{3} > \alpha > -1) \simeq 0.659$, $p_c(-1 > \alpha > -3) \simeq 0.909$, and $p_c(-3 > \alpha) \simeq 0.945$. It is clear that these results are physically unacceptable as there is no reason for such a complex sequence of nonuniform convergences through which large classes of critical lines share, at $T=0$, single points. Consequently, we consider this fact as a

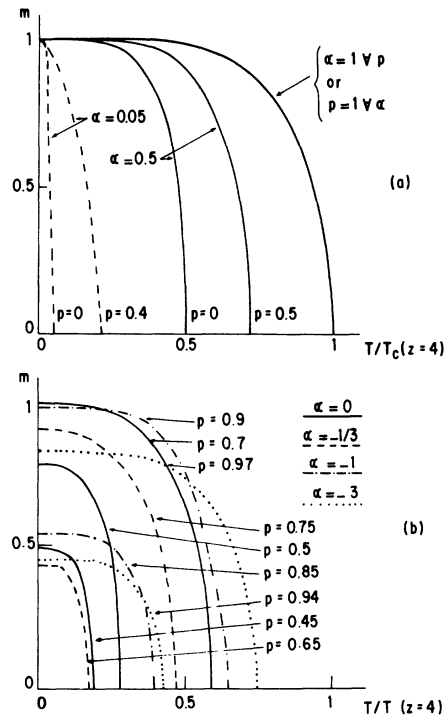


FIG. 6. Fixed-concentration sections of the family of surfaces represented in Fig. 4 for various values of $\alpha \equiv J'_0/J_0$ (a) $\alpha > 0$, (b) $\alpha \leq 0$.

mathematical artifact of the present approximation. Within this context, $\alpha = -\frac{1}{3}, -1, -3$ constitute exceptional points. Let us conclude our discussion of the square lattice phase diagram by saying that, excepting for the low-temperature region associated with almost all negative values of α , the present prediction (Fig. 3) can be given a reasonable degree of qualitative (and to a certain extent quantitative) confidence. In what concerns our results for the magnetization m , we indicate in Fig. 4 the evolution of $m(t, p)$ as a function of α ; in Figs. 5 and 6 we present illustrative sections of the same surface.

$$\begin{aligned}
 p^6 \left[\tanh \frac{6}{t} + 4 \tanh \frac{4}{t} + 5 \tanh \frac{2}{t} \right] + 10p^5(1-p) \left[\tanh \frac{5}{t} + 3 \tanh \frac{3}{t} + 2 \tanh \frac{1}{t} \right] \\
 + 40p^4(1-p)^2 \left[\tanh \frac{4}{t} + 2 \tanh \frac{2}{t} \right] + 80p^3(1-p)^3 \left[\tanh \frac{3}{t} + \tanh \frac{1}{t} \right] \\
 + 80p^2(1-p)^4 \tanh \frac{2}{t} + 32p(1-p)^5 \tanh \frac{1}{t} = \frac{16}{3}. \quad (32)
 \end{aligned}$$

The equation leads, in the limit $t \rightarrow 0$, to the bond-percolation critical probability $p_c \equiv p_c(\alpha=0) \simeq 0.2929$, which is to be compared with $p_c^{\text{series}} \simeq 0.247$,⁶⁹ $p_c^{\text{CPA}} = \frac{1}{3}$ (Ref. 70) (CPA is the coherent-potential approximation), and $p_c^{\text{MFA}} = 0$. We verify that, contrarily to what happens for the square lattice, $p_c(\alpha=0)$ is *higher* than p_c^{series} (assumed almost exact), and therefore the present framework now *understabilizes* the ferromagnetic phase. This is the first time in this work that we are facing a counterexample of the general tendency (of the present approximation) to overestimate the stability of the ferromagnetic phase. What happens is that the negligence of multispin correlations introduces a tendency towards ferromagnetic overstabilization

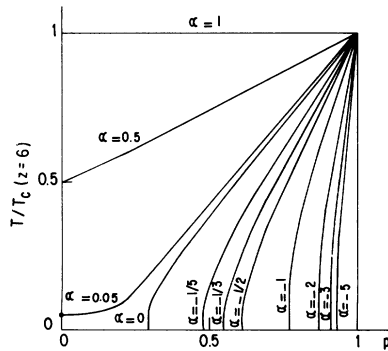


FIG. 7. Examples of critical lines (ferromagnetic-phase-stability limit) associated with the quenched random-bond Ising model in simple cubic lattice ($z=6$) for both competing ($\alpha \equiv J'_0/J_0 < 0$) and noncompeting ($\alpha \geq 0$) cases.

3. Simple cubic lattice ($z=6$)

Herein we consider $J'_1 = J'_2 = J'_3 \equiv J'_0 \leq J_1 = J_2 = J_3 \equiv J_0$ ($\alpha \equiv J'_0/J_0$). The associated phase diagram for $\alpha \geq 0$ (noncompeting case) is presented in Ref. 52. In the present section we extend this diagram to $\alpha < 0$ (competing case) and discuss the magnetization as function of temperature and J_0 -bond concentration as well as the phase diagram in the (p, t, α) space (see Fig. 7). The critical line associated with the bond-diluted model ($\alpha=0$) is given by

zation which is, however, *strongly modulated* by topological considerations, and *can even be reversed*. The situation is illustrated in Fig. 8, where several $z=4$ and $z=6$ cases are presented. By remembering that a Bethe tree corresponds to an infinite effective lattice dimensionality we remark that (i) the present approximation has an overall tendency to overestimate (underestimate) the ferromagnetic stability for sufficiently low (high) dimensionalities; (ii) the overestimation tendency increases with temperature (or equivalently the underestimation tendency decreases with temperature), and consequently eventual “crossings” (see three examples in Fig. 8) are *a priori* expected to occur in such a way that $T_c(z) > T_c^{\text{exact}}$ and $p_c(z) < p_c^{\text{exact}}$; (iii) excepting the MFA, the dispersion of the results associated with a given coordination number z tends to be smaller at low temperatures (i.e., the incompleteness of z as topological information tends to be less crude at low temperatures). It is possible to partially overcome these types of difficulties by incorporating^{45,46} into the present formalism multispin correlation effects (this is, however, out of the scope of this work). Equation (32) also yields

$$\frac{1}{T_c(1)} \left. \frac{dT_c(p)}{dp} \right|_{p=1} \simeq 1.200 \quad (33)$$

and

$$(1-p_c) \left. \frac{de^{-2/t_c(p)}}{dp} \right|_{p=p_c} \simeq 1.596. \quad (34)$$

The first of these results is to be compared with

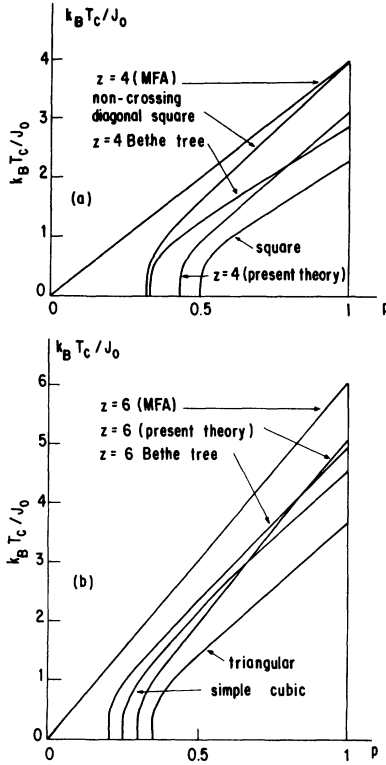


FIG. 8. Comparison between quenched bond-diluted Ising ferromagnet critical lines associated with typical $z=4$ (a) and $z=6$ (b) cases. The MFA line is given by $k_B T_c^{\text{MFA}}/J_0 = zp$; the z -coordinated Bethe tree line is exact (Refs. 40, 71, 72) $\{k_B T_c^{\text{exact}}(1)/J_0 = 2/\ln[z/(z-2)]$ and $p_c^{\text{exact}} = 1/(z-1)\}$; the $z=4$ ($z=6$) present theory line is given by Eq. (41) [Eq. (51)]; the noncrossing diagonal square lattice line is almost exact (Ref. 73) $[k_B T_c^{\text{exact}}(1)/J_0 = 3.93 \dots$ (Ref. 74) and $p_c^{\text{exact}} = 0.321$]; the square lattice line is almost exact (Refs. 29, 40, 73) $[k_B T_c^{\text{exact}}(1)/J_0 = 2.269 \dots$ and $p_c^{\text{exact}} = \frac{1}{2}$ (Ref. 63)]; the triangular lattice line is almost exact (Ref. 75) $[k_B T_c^{\text{exact}}(1)/J_0 = 3.64 \dots$ (Ref. 74) and $p_c^{\text{exact}} = 0.347 \dots$ (Ref. 63)]; the simple cubic lattice line is a reasonable approximation (Ref. 39) $[k_B T_c^{\text{series}}(1)/J_0 \simeq 4.5112$ (Ref. 57) and $p_c^{\text{series}} \simeq 0.247$ (Ref. 69)].

the approximate values 1.060 (from Ref. 21), 0.881, and 0.900 (from Ref. 39); the second one is to be compared with the approximate values 1.770 (from Ref. 21), 2.176, and 1.811 (from Ref. 39). As before, we remark that the present simple effective-field theory provides the (possibly) exact asymptotic forms for the critical line *simultaneously* in both limits $T \rightarrow 0$ and $p \rightarrow 1$. Furthermore, the critical lines associated with $0 < \alpha < 1$ present (see Fig. 7) the expected nonuniform convergence in the limit $\alpha \rightarrow 0$.

Let us now discuss the phase diagrams associated

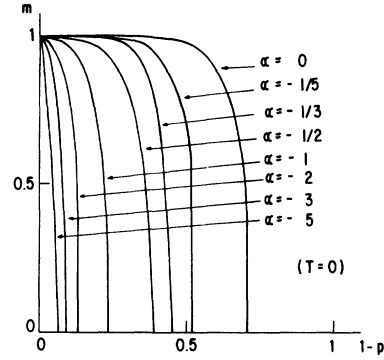


FIG. 9. $T=0$ section of the surfaces of the $z=6$ magnetization function $m(t,p)$ for various values of $\alpha \equiv J'_0/J_0$.

with $\alpha < 0$. At $T=0$ we obtain the following results: $p_c(\alpha = -\frac{1}{5}) \simeq 0.4818$, $p_c(\alpha = -\frac{1}{3}) \simeq 0.5531$, $p_c(\alpha = -\frac{1}{2}) \simeq 0.6084$, $p_c(\alpha = -1) = \frac{23}{30}$, $p_c(\alpha = -2) \simeq 0.8663$, $p_c(\alpha = -3) \simeq 0.9061$, and $p_c(\alpha = -5) \simeq 0.9342$.

For negative values of α other than $-\frac{1}{5}$, $-\frac{1}{3}$, $-\frac{1}{2}$, -1 , -2 , -3 , and -5 the present treatment provides, in the limit $T \rightarrow 0$, the same curious situa-

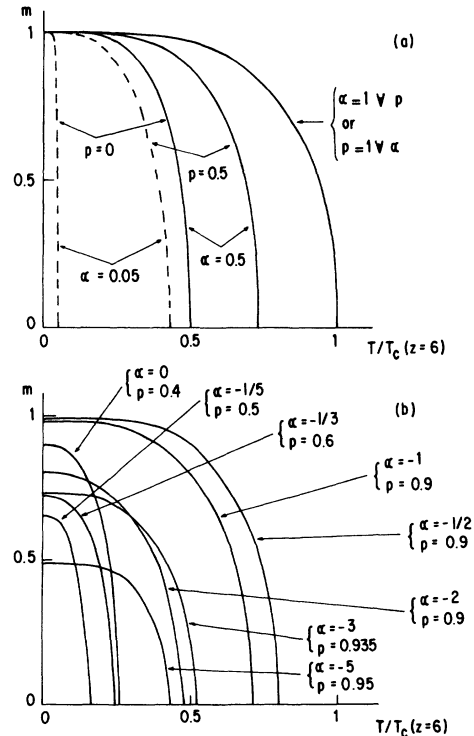


FIG. 10. Fixed-concentration sections of the surfaces of the $z=6$ magnetization function $m(t,p)$ for various values of $\alpha \equiv J'_0/J_0$. (a) $\alpha > 0$; (b) $\alpha \leq 0$.

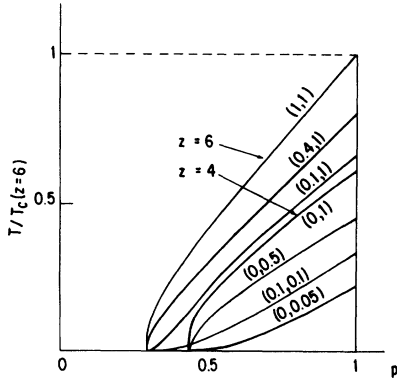


FIG. 11. Examples of critical lines associated with the quenched bond-diluted anisotropic model; the pairs of numbers represent $(\gamma_1; \gamma_2)$, where $\gamma_i \equiv J_i/J_3$ ($i=1,2$). Although not graphically visible in all the cases, all the critical lines satisfy $(dT/dp)_{p=p_c(z)} = \infty$. The (1;1) and (0.4;1) lines correspond to region VII of Fig. 1(c) and are clearly $d=3$; the (0.1;1) line can be considered as belonging to region V of the same figure and exhibits the $d=2 \leftrightarrow d=3$ crossover; the (0;1) and (0;0.5) lines correspond to region III and are clearly $d=2$; the (0;0.05) line can be considered as belonging to region II and exhibits the $d=1 \leftrightarrow d=2$ crossover; finally the (0.1;0.1) line can be considered as belonging to region VI and exhibits the $d=1 \leftrightarrow d=3$ crossover. Within the present scale it is impossible to satisfactorily represent the region IV (let us say $\gamma_1=0.005$ and $\gamma_2=0.1$) in order to exhibit the $d=1 \leftrightarrow d=2 \leftrightarrow d=3$ crossover; however, it corresponds to a line whose critical temperature practically vanishes at $p=p_c(z=4)$ but nevertheless exhibits a thin tail which strictly vanishes only at $p=p_c(z=6)$.

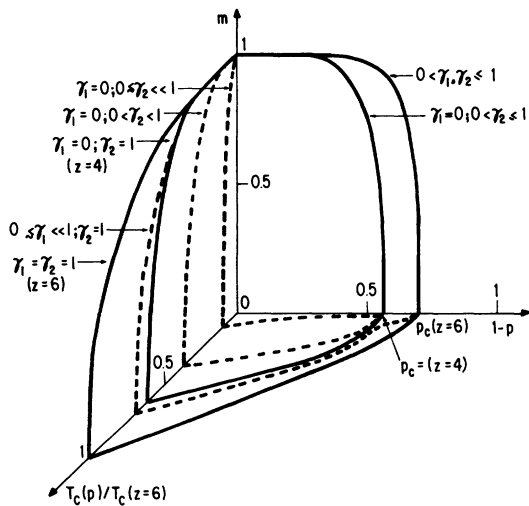


FIG. 12. Evolution of the magnetization $m(t,p)$ as function of (γ_1, γ_2) , where $\gamma_i \equiv J_i/J_3$ ($i=1,2$), for the quenched bond-diluted anisotropic $z=6$ model. The two vanishing-temperature curves are universal. The $d=1 \leftrightarrow d=2$ and $d=2 \leftrightarrow d=3$ crossovers are exhibited.

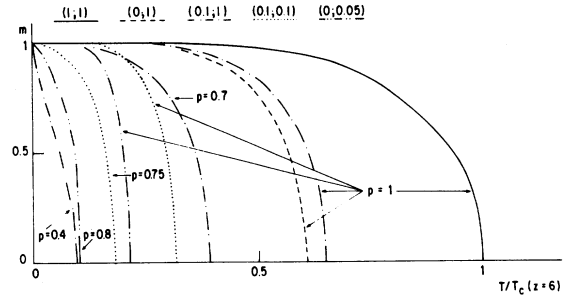


FIG. 13. Fixed-concentration sections of the family of surfaces represented in Fig. 12 for various values of $(\gamma_1; \gamma_2)$.

tion obtained in the $z=4$ case, namely, that large classes of critical lines share (at $T=0$) single points. As before we consider this result as mathematical artifact of the present approximation. Let us conclude our discussion of the simple cubic lattice phase diagram by saying that, excepting for the low-temperature region associated with almost all negative values of α , the present result (Fig. 7) can be given a reasonable degree of qualitative (and to a certain extent quantitative) confidence.

Our results for the $z=6$ magnetization $m(t,p)$ evolve, as a function of α , similarly to the $z=4$ case (see Fig. 4); in Figs. 9 and 10 we present illustrative sections of the $z=6$ surfaces $m(t,p)$ for different values of α .

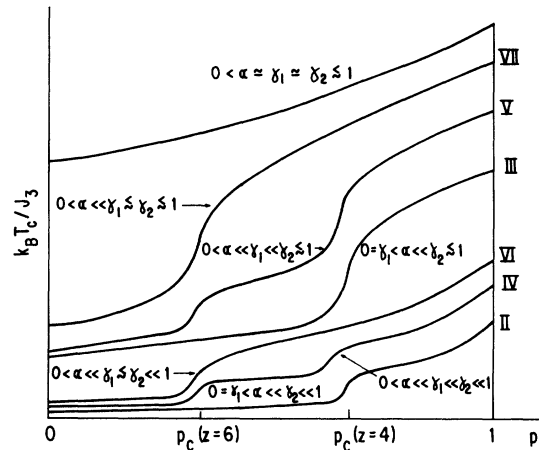


FIG. 14. Selected critical lines (*out of scale*) associated with the quenched random-bond anisotropic model with $J'_i/J_3 \equiv \alpha$ ($i=1,2,3$) and $0 \leq \gamma_1 \leq \gamma_2 \leq 1$ with $\gamma_i \equiv J_i/J_3$ ($i=1,2$). The roman numerals refer to the regions defined in Fig. 1(c). Notice the richness of crossovers [in particular the IV line exhibits the $d=1 \leftrightarrow d=2 \leftrightarrow d=3 \leftrightarrow$ (nondilute) crossover].

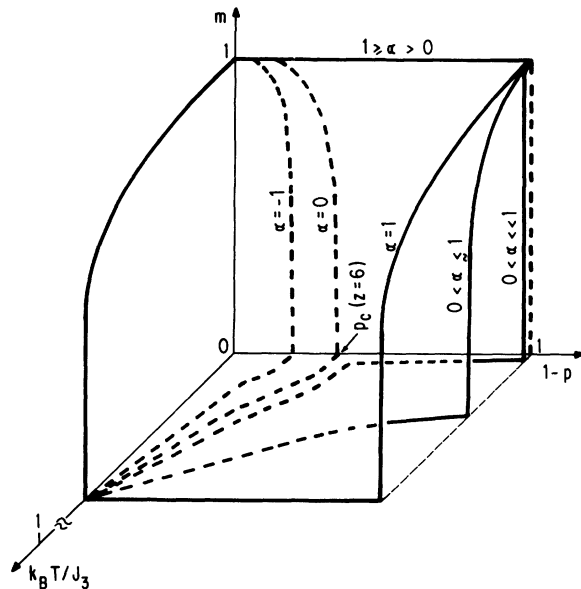


FIG. 15. Out of scale illustration of the influence of $\alpha \equiv J'_i/J_i$ ($i=1,2,3$) on the magnetization $m(t,p)$ for the quenched random-bond model in the anisotropic $z=6$ model. The present example refers to $0 < \gamma_1 \lesssim \gamma_2 \ll 1$ [$\gamma_i \equiv J_i/J_3$ ($i=1,2$)]. Notice, for $0 < \alpha \ll 1$, the $d=1 \leftrightarrow d=3 \leftrightarrow$ (nondilute) crossover.

C. Bond-diluted anisotropic models

Herein we consider $J'_1=J'_2=J'_3=0$ (hence $\alpha_1=\alpha_2=\alpha_3=0$) and $0 \leq J_1 \leq J_2 \leq J_3$ (hence $0 \leq \gamma_1 \leq \gamma_2 \leq 1$). The magnetization is given by Eq. (13). Equation (14) provides the phase diagram in the (p,t,γ_1,γ_2) space. Selected critical lines are presented in Fig. 11, where, in particular, we can note the $d=1 \leftrightarrow d=2$, $d=1 \leftrightarrow d=3$, and $d=2 \leftrightarrow d=3$ crossovers. The evolution of the magnetization $m(t,p)$ as function of (γ_1,γ_2) is represented in Fig. 12, and illustrative fixed-concentration sections of this family of surfaces are represented in Fig. 13.

D. Random-bond anisotropic models

Herein we consider (quite briefly) our last particular case, namely, $J'_1/J_1=J'_2/J_2=J'_3/J_3$ (hence $\alpha_1=\alpha_2=\alpha_3 \equiv \alpha \leq 1$) and $0 \leq J_1 \leq J_2 \leq J_3 > 0$ (hence $0 \leq \gamma_1 \leq \gamma_2 \leq 1$). The most interesting situations appear for $0 < \alpha \ll 1$; however, the numerical and appropriate graphical scales are such that, instead of presenting quantitative results, we shall restrict ourselves to the qualitative description of the phase diagram: Its main properties are illustrated in Fig. 14 (out of scale). Furthermore, the evolution of the magnetization $m(t,p)$ with α is qualitatively indicat-

ed in Fig. 15 (out of scale) for the model $0 < \gamma_1 \lesssim \gamma_2 \ll 1$.

IV. CONCLUSION

We have discussed the phase diagram (stability limit of the ferromagnetic phase) and the magnetization of a quite general random system, namely, the quenched bond-mixed first-neighboring spin- $\frac{1}{2}$ Ising model (with both competing and noncompeting interactions) on an anisotropic simple cubic lattice. To perform these calculations we have adapted to the present situation an effective-field framework (based on the use of a convenient differential operator) introduced by Honmura and Kaneyoshi in 1978. This formalism is, from the analytical standpoint, almost as simple as the standard mean-field approximation (and, because of negligence of multispin correlations, shares with it the fact that the critical exponents are all Landau-type, and the related fact that the topology of the system is only partially taken into account, essentially through the coordination number); nevertheless, we verify that its results are quite superior in at least two important senses, as it is capable of providing (i) vanishing critical temperature for one-dimensional systems, and (ii) expected nonuniform convergences in the highly diluted and highly anisotropic limits. We have illustrated both properties through many examples in which interesting crossovers [$d=1 \leftrightarrow d=2$, $d=1 \leftrightarrow d=3$, $d=2 \leftrightarrow d=3$, $d=1 \leftrightarrow d=2 \leftrightarrow d=3$, (dilute)-(nondilute) as well as mixed situations] occur. Instead of recalling here the main results associated with the variety of physically important particular cases considered herein, we rather refer the reader to Figs. 1, 3, 4, 7, 11, 12, 14, and 15 where the most relevant situations are exhibited.

The calculations of several particular values and various asymptotic behaviors (essentially in the low-temperature, quasi-pure- and high-anisotropies limits) and, whenever is possible, their comparison with those available in literature (and obtained through other techniques) supports the belief that the results provided by the present framework can be given qualitative (and to a certain extent quantitative) confidence. In a forthcoming paper we intend to discuss effects which have not been analyzed herein, namely, those due to anisotropy in the bond-occupancy probabilities.

ACKNOWLEDGMENTS

It is with pleasure that we acknowledge interesting remarks from I. P. Fittipaldi. Work partially supported by Conselho Nacional de Desenvolvimento Científico e Tecnológico (Brazilian Agency).

- ¹J. M. Baker, J. A. J. Lourens, and R. W. H. Stevenson, *Proc. Phys. Soc.* **77**, 1038 (1961).
- ²R. J. Birgeneau, R. A. Cowley, G. Shirane, and H. J. Guggenheim, *Phys. Rev. Lett.* **37**, 940 (1976).
- ³R. A. Cowley, G. Shirane, R. J. Birgeneau, and H. J. Guggenheim, *Phys. Rev. B* **15**, 4292 (1977).
- ⁴T. E. Wood and P. Day, *J. Phys. C* **10**, L333 (1977).
- ⁵M. Suzuki and H. Ikeda, *J. Phys. C* **11**, 3679 (1978).
- ⁶L. Bevaart, E. Frikkee, J. V. Lebesque, and L. J. de Jongh, *Phys. Rev. B* **18**, 3376 (1978).
- ⁷K. Katsumata, M. Kobayashi, T. Sató, and Y. Miyako, *Phys. Rev. B* **19**, 2700 (1978).
- ⁸P. Wong and P. M. Horn, *Bull. Am. Phys. Soc.* **24**, 363 (1979).
- ⁹S. Oseroff, R. Calvo, and W. Girit, *J. Appl. Phys.* **50**, 7738 (1979).
- ¹⁰K. Adachi, K. Sató, M. Matsuura, and M. Ohashi, *J. Phys. Soc. Jpn.* **29**, 323 (1970).
- ¹¹W. Y. Ching and D. L. Huber, *Phys. Rev. B* **13**, 2962 (1976).
- ¹²D. P. Landau, *Phys. Rev. B* **22**, 2450 (1980).
- ¹³A. B. Harris, *J. Phys. C* **7**, 1671 (1974).
- ¹⁴R. V. Ditzian and L. P. Kadanoff, *Phys. Rev. B* **19**, 4631 (1979).
- ¹⁵R. Bidaux, J. P. Carton, and G. Sarma, *J. Phys. A* **9**, L87 (1976).
- ¹⁶R. A. Tahir-Kheli and R. J. Elliott, *J. Phys. C* **10**, 275 (1977).
- ¹⁷A. R. McGurn and M. F. Thorpe, *J. Phys. C* **11**, 3667 (1978).
- ¹⁸M. F. Thorpe and A. R. McGurn, *Phys. Rev. B* **20**, 2142 (1979).
- ¹⁹E. J. S. Lage and R. B. Stinchcombe, *J. Phys. C* **12**, 1319 (1979).
- ²⁰B. Frank and N. Jan, *J. Phys. C* **12**, 3779 (1979).
- ²¹L. Turban, *Phys. Lett. A* **75**, 307 (1980).
- ²²F. G. Brady Moreira, I. P. Fittipaldi, and R. B. Stinchcombe, *J. Phys. C* **14**, 4415 (1981).
- ²³E. Domany, *J. Phys. C* **11**, L337 (1978).
- ²⁴T. Oguchi and Y. Ueno, *J. Phys. Soc. Jpn.* **44**, 1449 (1978).
- ²⁵R. Fisch, *J. Stat. Phys.* **18**, 111 (1978).
- ²⁶H. Nishimori, *J. Phys. C* **12**, L905 (1979).
- ²⁷B. W. Southern, *J. Phys. C* **13**, L285 (1980).
- ²⁸A. Aharony and M. J. Stephen, *J. Phys. C* **13**, L407 (1980).
- ²⁹C. Tsallis, *J. Phys. C* **14**, L85 (1981).
- ³⁰T. K. Bergstresser, *J. Phys. C* **10**, 3831 (1977).
- ³¹S. Kirkpatrick, *Phys. Rev. B* **15**, 1533 (1977).
- ³²C. Jayaprakash, E. K. Riedel, and M. Wortis, *Phys. Rev. B* **18**, 2244 (1978).
- ³³W. Klein, H. E. Stanley, P. J. Reynolds, and A. Coniglio, *Phys. Rev. Lett.* **41**, 1145 (1978).
- ³⁴F. Shibata and M. Asou, *J. Phys. Soc. Jpn.* **46**, 1075 and 1083 (1979).
- ³⁵J. M. Yeomans and R. B. Stinchcombe, *J. Phys. C* **12**, L169 (1979); **12**, 347 (1979); **13**, 85 (1980).
- ³⁶M. Schwartz and S. Fishman, *Physica A* **104**, 115 (1980).
- ³⁷C. Tsallis and S. V. F. Levy, *J. Phys. C* **13**, 465 (1980).
- ³⁸S. V. F. Levy, C. Tsallis, and E. M. F. Curado, *Phys. Rev. B* **21**, 2991 (1980).
- ³⁹N.-C. Chao, G. Schwachheim, and C. Tsallis, *Z. Phys. B* **43**, 305 (1981).
- ⁴⁰A. C. N. de Magalhães and C. Tsallis, *J. Phys. (Paris)* **42**, 1515 (1981).
- ⁴¹A. R. McGurn, *J. Phys. C* **13**, 1055 (1980).
- ⁴²R. Honmura and T. Kaneyoshi, *Prog. Theor. Phys.* **60**, 635 (1978); *J. Phys. C* **12**, 3979 (1979).
- ⁴³F. C. Sá Barreto and I. P. Fittipaldi, *Rev. Bras. Fis.* **11**, 745 (1981).
- ⁴⁴H. B. Callen, *Phys. Lett.* **4**, 161 (1963).
- ⁴⁵T. Kaneyoshi, I. P. Fittipaldi, R. Honmura, and T. Manabe, *Phys. Rev. B* **24**, 481 (1981).
- ⁴⁶G. B. Taggart and I. P. Fittipaldi, *Phys. Rev. B* **25**, 7026 (1982).
- ⁴⁷F. C. Sá Barreto and I. P. Fittipaldi, *Ferroelectrics* **39**, 1103 (1981).
- ⁴⁸R. Honmura, A. F. Khater, I. P. Fittipaldi, and T. Kaneyoshi, *Solid State Commun.* **41**, 385 (1982).
- ⁴⁹T. Kaneyoshi, I. P. Fittipaldi, and H. Beyer, *Phys. Stat. Solidi B* **102**, 393 (1980).
- ⁵⁰J. R. de Almeida, I. P. Fittipaldi, and F. C. Sá Barreto, *J. Phys. C* **14**, L403 (1981).
- ⁵¹I. P. Fittipaldi, C. Tsallis, and E. F. Sarmiento, *Solid State Commun.* **44**, 777 (1982).
- ⁵²E. F. Sarmiento, C. Tsallis, and I. P. Fittipaldi, *J. Magn. Magn. Mater.* (in press).
- ⁵³T. Kaneyoshi and H. Beyer, *J. Phys. Soc. Jpn.* **49**, 1306 (1980).
- ⁵⁴K. Sakata, E. F. Sarmiento, I. P. Fittipaldi, and T. Kaneyoshi, *Solid State Commun.* **42**, 13 (1982).
- ⁵⁵N. Matsudaira, *J. Phys. Soc. Jpn.* **35**, 1593 (1973).
- ⁵⁶L. Onsager, *Phys. Rev.* **65**, 117 (1944).
- ⁵⁷J. Zinn-Justin, *J. Phys. (Paris)* **40**, 969 (1979).
- ⁵⁸F. Zernike, *Physica (Utrecht)* **7**, 565 (1940).
- ⁵⁹H. Mamada and F. Takamo, *J. Phys. Soc. Jpn.* **25**, 675 (1968).
- ⁶⁰D. C. Mattis, *Phys. Rev. B* **19**, 4737 (1979).
- ⁶¹G. Paul and H. E. Stanley, *Phys. Rev. B* **5**, 2578 (1972).
- ⁶²J. Oitmaa and I. G. Enting, *Phys. Lett. A* **36**, 91 (1971).
- ⁶³M. F. Sykes and J. Essam, *Phys. Rev. Lett.* **10**, 3 (1963).
- ⁶⁴E. Domany, *J. Phys. C* **12**, L119 (1979).
- ⁶⁵S. Katsura, S. Inawashiro, and S. Fujiki, *Physica A* **99**, 193 (1979).
- ⁶⁶M. Gabay and T. Garel, *Phys. Lett. A* **65**, 135 (1978).
- ⁶⁷J. Vannimenus and G. Toulouse, *J. Phys. C* **10**, L537 (1977).
- ⁶⁸G. Grinstein, C. Jayaprakash, and M. Wortis, *Phys. Rev. B* **19**, 260 (1979).
- ⁶⁹D. S. Gaunt and H. Ruskin, *J. Phys. A* **11**, 1369 (1978).
- ⁷⁰F. G. Brady-Moreira and I. P. Fittipaldi, *J. Appl. Phys.* **50**, 1726 (1979).
- ⁷¹B. W. Southern and M. F. Thorpe, *J. Phys. C* **12**, 5351 (1979).

⁷²T. Horiguchi and T. Morita, *J. Phys. A* **13**, L71 (1980).

⁷³C. Tsallis and A. C. N. de Magalhães, *J. Phys. (Paris)* **42**, L227 (1981).

⁷⁴I. Syozi, *Phase Transitions and Critical Phenomena*, edited by C. Domb and M. S. Green (Academic, Lon-

don, New York, 1972), Vol. 1, p. 270, and references therein.

⁷⁵A. C. N. de Magalhães, G. Schwachheim, and C. Tsallis, *J. Phys. C* (in press).